Astron. Astrophys. 303, 795–800 (1995)

ASTRONOMY AND ASTROPHYSICS

The companion of Z Canis Majoris detected in the visible*

E. Thiébaut[1], J. Bouvier[2], A. Blazit[3], D. Bonneau[3], F.-C. Foy[1], and R. Foy[1]

[1] Centre de Recherche Astronomique de Lyon, CNRS UMR 142 and Observatoire de Lyon, 9 av. Charles André, F-69561 Lyon, France
[2] Observatoire de Grenoble, CNRS URA 708, France
[3] Observatoire de la Côte d'Azur, Département A. Fresnel, CNRS URA 1361, France

Received 15 February 1995 / Accepted 18 April 1995

Abstract. We report the detection in the visible of the companion of the FU Orionis star Z Canis Majoris discovered in the infrared by Koresko et al. (1991). At 730 nm and 656 nm, the companion of Z CMa appears to be much brighter than predicted by the model of Koresko et al. (1991). We argue that the excess flux in the visible is due to scattered light from the companion. This interpretation agrees with the results of the spectropolarimetric study of the Z CMa system by Whitney et al. (1993).

Key words: stars: Z CMa; pre-main sequence – binaries: visual – accretion disks – techniques: interferometric

1. Introduction

Z Canis Majoris (Z CMa) is a FU Orionis star which has been found to be double in the infrared by Koresko et al. (1991, hereinafter referred as KBGMN). Stars of this kind are thought to be young stellar object in an active state whose luminosity is dominated by the contribution of an accretion disk (e.g., Hartmann et al. 1989). KBGMN were able to resolve the northwestern component (Z CMa NW) of the system which lies 0.″1 away from the southeastern one (Z CMa SE) and their measurements at different infrared wavelengths (1.27, 1.65, 2.2, 3.28, 4.05 and 4.8 μm) allowed them to derive a low resolution photometric spectrum for each component. In order to explain the shape of these spectra combined with IRAS data and with Herbst et al.'s (1987) photometric measurements of the integrated system at visible wavelengths, they proposed a three component model for Z CMa:

1. The spectrum of Z CMa SE is that of a FU Orionis star; it is dominated by the contribution of the accretion disk and accounts for the visible and UV fluxes.
2. Z CMa NW is an optically thick sphere of in-falling or outflowing dust around a bright object (a star or a FU Orionis accretion disk) which provides the energy needed to heat the dust. The spectrum of this component is that of a black body and accounts for most of the near infrared flux.
3. An accretion disk wide enough ($\geq$400AU) to surround the two stellar-like components. This third component is needed to explain the far infrared spectrum. In addition to viscous heating, re-processing of Z CMa SE flux in a flared disk may explain the flatness of the far IR spectrum.

Haas et al. (1993) observed a variability in the luminosity of the two components from epoch 1986.72 to epoch 1990.73 in the H and K bands. They argue that the independent brightness fluctuations of Z CMa SE and Z CMa NW provides additional support to their stellar nature, the fluctuations being ascribed to accretion bursts. This variability was confirmed by Roddier et al. (1994) who carried out observations at 1.28 μm and 1.65 μm with their adaptive optics system at the 3.6m CFH telescope and found at the latter wavelength that the formerly brighter component had become the fainter one. Malbet et al. (1993) claimed that they have directly imaged the large accretion disk (*i.e.* the third component in the model of KGBMN) by means of adaptive optics. This detection has not yet been confirmed by infrared speckle imaging (Tessier et al. 1994).

The detection at visible wavelengths of the so-called *infrared* companion (Z CMa NW) discovered by KBGMN was reported independently by Thiébaut (1994a) and by Barth et al. (1994). We present in Sect. 2 a detailed account of the speckle interferometry analysis of photon counting data acquired in the visible at the 3.60 m telescope of the CFH, which have allowed us to clearly resolve the companion at 730 and 656 nm. In Sect. 3, we discuss the implications of our flux ratio measurements of each component of the system for the models proposed so far to account for Z CMa's peculiar spectral energy distribution.

Send offprint requests to: E. Thiébaut

* Based on observations collected at the Canada-France-Hawaii Telescope operated by the National Research Council of Canada, the Centre National de la Recherche Scientifique de France and the University of Hawaii.

Table 1. Journal of observations: BD-11°1761 is the reference for Z CMa, λ and $\Delta\lambda$ are the wavelength and the bandwidth

object	epoch	λ (nm)	$\Delta\lambda$ (nm)	observing time (s)
Z CMa	1989.84012	656	28	124
BD-11°1761	1989.84013	656	28	154
Z CMa	1989.84551	730	28	243
BD-11°1761	1989.84553	730	28	653
Z CMa	1989.84556	730	28	374
BD-11°1761	1989.84558	730	28	158

2. Observations and results

We observed Z CMa at the CFH 3.60 m telescope during two nights in November 1989 (see Table 1). We used the speckle-graph described by Foy (1988b) and a CP40 photon counting camera (see Blazit 1987; Foy 1988a). We used BD-11°1761 as a reference star for the calibration of the speckle interferometry transfer function. Owing to the camera's limited field of view ($\sim 1''.5 \times 1''.5$), about 20 % of the short exposure frames had to be rejected because of tracking errors. The mean flux recorded in each channel of the photon counting camera per 20 ms integration was $\sim$ 70 photons for the object and $\sim$ 30 photons for the reference. During the observations, the seeing was $\sim 1''$.

We used the cross-correlation method described by Thiébaut (1994b) to compute the power spectrum of Z CMa avoiding the so-called *photon counting hole* (Foy 1988b). Besides, we obtained the Fourier phase of Z CMa from bispectrum analysis (*e.g.* Weigelt 1977 and Wirnitzer 1985). For that we used a two-channel bispectrum method (Thiébaut 1994a) to avoid, again, the degradation due to the photon counting defect (Hofmann 1993). In spite of the poor signal-to-noise ratio of the reconstructed Fourier phase, we were able to restore an image of Z CMa (see Fig. 1) using the method proposed by Thiébaut (1994a) and mainly based on the power spectrum. This method consists in searching for the object brightness distribution $o(\boldsymbol{x})$ which minimizes the quantity:

$$\epsilon = \sum_{u} w(\boldsymbol{u}) \left[\langle |S(\boldsymbol{u})|^2 \rangle \, |O(\boldsymbol{u})|^2 - \langle |I(\boldsymbol{u})|^2 \rangle \right]^2 + \mu \sum_{u} ||\boldsymbol{u}||^2 \, |O(\boldsymbol{u})|^2 \quad (1)$$

where $O(\boldsymbol{u})$ is the Fourier transform of $o(\boldsymbol{x})$, $I(\boldsymbol{u})$ and $S(\boldsymbol{u})$ are the Fourier transforms of the specklegrams of the object and of its reference respectively. The weighting function $w(\boldsymbol{u})$ is choosen as:

$$w(\boldsymbol{u}) = \begin{cases} 1/\mathrm{Var}(|I(\boldsymbol{u})|^2) & \text{if } r_0/\lambda \ll ||\boldsymbol{u}|| \leq u_{\mathrm{eff}} \\ 0 & \text{otherwise} \end{cases} \quad (2)$$

where u_{eff} is an effective cut-off frequency which depends on the noise level (and is less than the diffraction limit) and where the condition $r_0/\lambda \ll ||\boldsymbol{u}||$ allows one to avoid the fitting of the low frequency part of the power spectrum which is poorly calibrated because of seeing fluctuations (Christou et al. 1985).

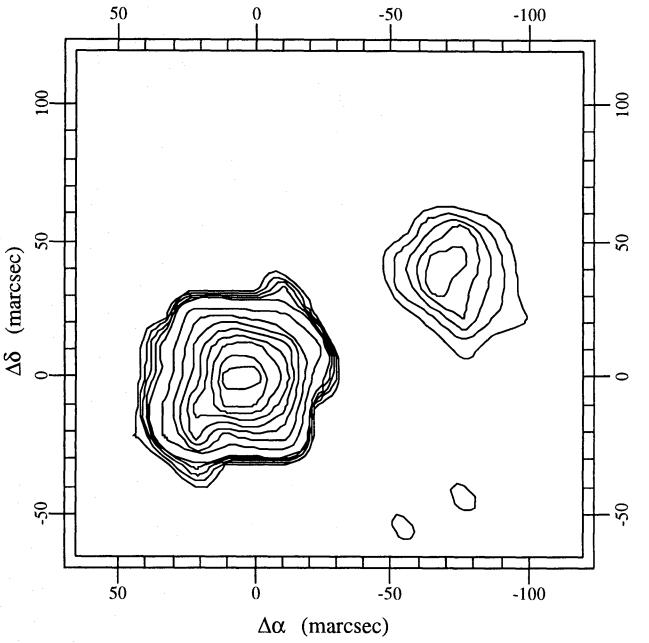

Fig. 1. Image of Z CMa restored from our photon counting data at 730 nm. North is up, east is left; the isocontours are 2%, 4%, 6%, 8%, 10%, 20%, 30%, 40%, 50%, 60%, 70%, 80%, and 90% of the peak intensity (see text for details about the restoration method)

In the right hand side of Eq. (1), the first term enforces compatibility of the model, *i.e.* $o(\boldsymbol{x})$, with the data, while the second term enforces the smoothness of $o(\boldsymbol{x})$ and is used to regularize the restoration problem (Demoment 1989). We set the value of the hyperparameter μ so that the data are not overfitted by the model: μ is adjusted so as to have

$$\sum_{u} w(\boldsymbol{u}) \left[\langle |S(\boldsymbol{u})|^2 \rangle \, |O(\boldsymbol{u})|^2 - \langle |I(\boldsymbol{u})|^2 \rangle \right]^2 \simeq N$$

where N is the number of spatial frequencies taken into account in the sum. Furthermore, since a brightness distribution must be positive, we apply a strict constraint of positivity (Thiébaut & Conan 1995) by rewritting the model as $o(\boldsymbol{x}) = \exp(\alpha(\boldsymbol{x}))$ and by fitting $\alpha(\boldsymbol{x})$ so as to minimize ϵ. This method for restoring an image has proven to be able to cope with low signal to noise ratio data and also with incomplete data but it leaves an ambiguity in the orientation of the restored image which is known modulo 180°. In order to remove this uncertainty, we used the Fourier phase (obtained from the bispectrum) and combined it with the Fourier modulus of the restored image. This gave us a noisy image which, however, clearly shows that the faintest component is the northwestern one. Figure 1 shows the image restored from the power spectra and with the good orientation.

Figure 1 clearly shows the "infrared" companion of Z CMa. Because this image was restored via a non-linear method, we fitted the parameters of the binary system (orientation, separation, and flux ratio) on the measured visibilities rather than on the image. The resulting parameters at 656 nm and 730 nm are listed in Table 2; there is a 2 mag difference between the

Table 2. Parameters for the binary system of Z CMa. The magnitude difference is $\Delta m = m_{\text{Z CMa NW}} - m_{\text{Z CMa SE}}$, and PA is the position angle of the northwestern component with respect to the southest one; consequently, we added 180° to the PA given by Koresko et al. (1991) and Haas et al. (1993)

source	epoch	wavelength	Δm	separation	PA
Thiébaut (1994a) and this paper	1989.84	730 ± 14 nm	2.3 ± 0.3	0.″110 ± 0.″007	294° ± 4°
this paper	1989.84	656 ± 14 nm	2.0 ± 0.7	0.″103 ± 0.″012	302° ± 8°
Barth et al. (1994)	1993.24	658 ± 27 nm	2.1	0.″100 ± 0.″008	305° ± 2°
		610 nm	2.2		
Koresko et al. (1991)	1989.94-1990.86	J	1.70 ± 0.53	0.″100 ± 0.″007	300° ± 4°
		H	1.07 ± 0.28		
		K	−0.88 ± 0.16		
		3.28 μm	−1.78 ± 1.12		
		4.05 μm	−2.00 ± 0.99		
		M	−2.07 ± 0.70		
Haas et al. (1993)	1986.72	H	0.87 ± 0.05	0.″100 ± 0.″010	302° ± 2°
	1987.69	H	1.00 ± 0.05		
	1988.73	H	1.11 ± 0.06		
	1990.87	H	1.08 ± 0.06		
Haas et al. (1993)	1987.12	K	−1.31 ± 0.07	0.″100 ± 0.″010	302° ± 2°
	1989.70	K	−0.76 ± 0.04		
	1990.87	K	−0.87 ± 0.05		
	1990.93	K	−0.50 ± 0.03		

secondary and the primary at the wavelengths of our observations. Table 2 shows that the separation and P.A. we measured are in fairly good agreement with the infrared measurements of KBGMN and Haas et al. (1993).

The bandwidth of our observations at 656 nm include the Hα line. There is no peculiar feature in the power spectrum at this wavelength, in addition to the fringe pattern due to the binarity. It means that there is no evidence for a bright jet emanating from any of the two components at a scale of a few tenths of AU. However, we wish to point out that: (i) the signal to noise ratio is low owing to the short integration time ($\sim 2\,RMmn$, Table 1) and results in comparatively large error bars in the measured parameters of the binary (see Table 2), and (ii) the bandwidth is 28 nm so that the dilution factor of the Hα emission is high.

3. Discussion

3.1. The nature of the southeast component

Figure 2 shows the spectral energy distribution (SED) of Z CMa from 0.36 to 100 μm. Following KBGMN, we have assuming that the UBV spectrum of Z CMa is dominated by Z CMa SE and we have used the UBVRI measurements of Herbst et al. 1987. Combining the total flux measured by Herbst et al. for the integrated system and the flux ratios between the two components of the system that we derived above, we computed the absolute flux of Z CMa SE and Z CMa NW at 730 nm and 656 nm. The SED was drawn taking into account an extinction $A_V = 0.81$ magnitude (Clariá 1974) and assuming a distance $D = 1150$ pc for the Canis Majoris association (Clariá 1974).

In order to find out if our measurements are consistent with the description of KGBMN who assume that Z CMa SE is a FU Ori object we have modelled the SED of a FU Orionis object following the T Tauri accretion disk model of Bertout et al. (1988): the optically thick disk is assumed to be flat and geometrically thin. We approximated the central star SED by a black body spectrum. Since the flux of a FU Orionis object is dominated by the accretion disk, this approximation has little effect on the inferred parameters. The thickness of the boundary layer between the star's surface and the disk is left as a free parameter in our fits. The emission of this layer usually dominates in the UV part of the spectrum. Because FU Orionis objects are known to be highly variable, it is important to note that our observations were carried out almost at the same epoch as the earliest speckle observations of KGBMN.

Using this FU Orionis model and fitting the observed SED of Z CMa SE from 0.36 to 5 μm, we deduce the following parameters for Z CMa SE:

$$L_{\text{acc}} = 1300 \pm 20\,L_\odot$$
$$R_\star = 13 \pm 1\,R_\odot$$

where $R_\star$ is the radius of the central star and L_{acc} is the accretion luminosity. The stellar luminosity is found to be negligible compared to the disk's luminosity, and thus does not contribute to the observed flux even at visible wavelengths. Similarly, the contribution of the boundary layer to the observed flux is found to be negligible. Figure 2 shows the good agreement between this model and the data for the SE component (model curve number (1) in Fig. 2).

Since, for our accretion disk model, the disk radiates half of the accretion power, we have: $L_{\text{disk}} = \frac{1}{2}L_{\text{acc}} \simeq 650\,L_\odot$ which is in agreement with the value obtained by KBGMN (ie. $L_{\text{disk}} \simeq 640\,L_\odot$). On the other hand, we obtain a rather different value for the inner disk radius: $13\,R_\odot$ in our fit against $20\,R_\odot$ in the fit of KBGMN. The disk luminosity is mainly determined by the infrared data. Since we use the same data as KBGMN at these

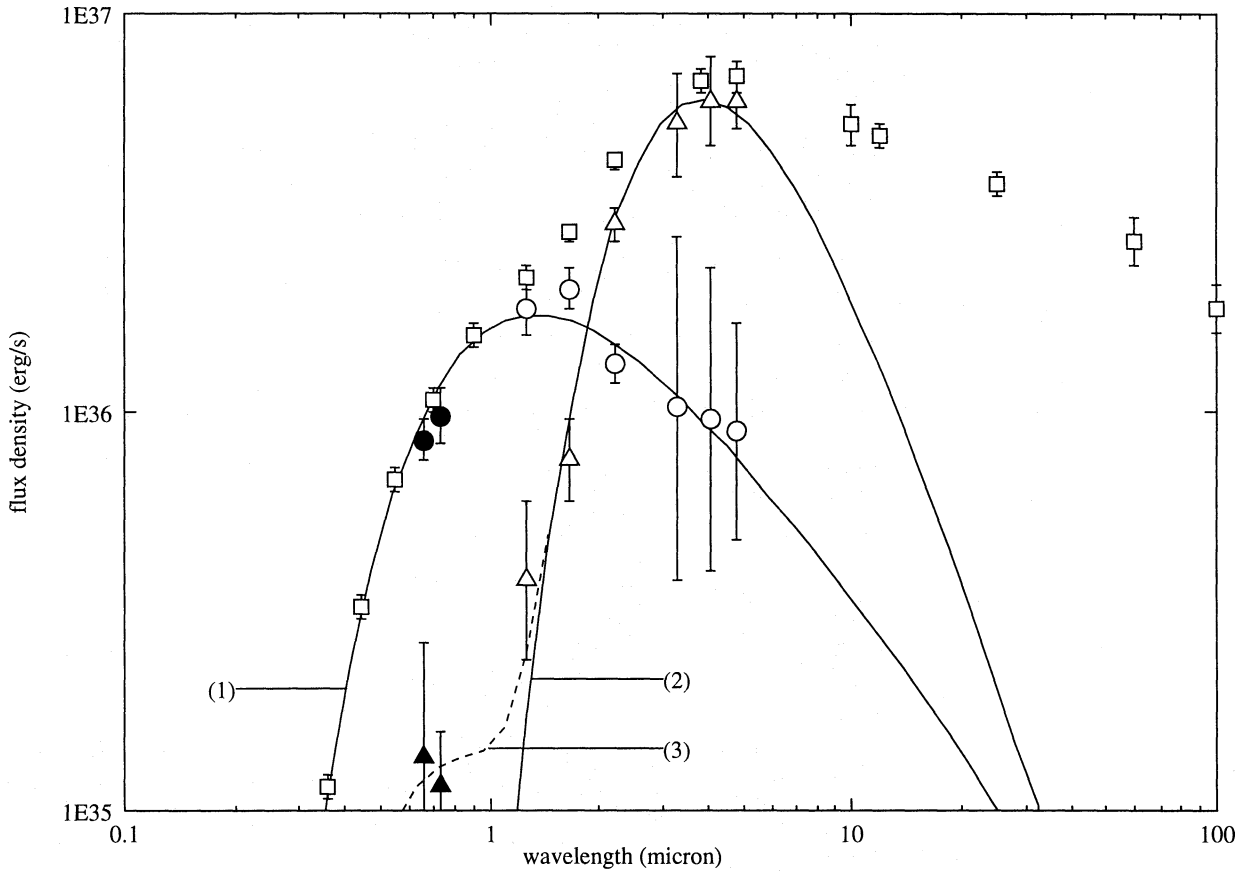

Fig. 2. Spectral energy distribution of the components of Z CMa: . and △ are for Z CMa SE and Z CMa NW, respectively, as measured by KBGMN; ∘ is for the total spectrum (Koresko et al. 1991, *IRAS Point Source Catalog* and Herbst et al. 1987); filled symbols are for our measurements at 730 nm and 656 nm. The curves show different model fits: (1) is the FU Orionis model for Z CMa SE, (2) is the sphere of dust model for Z CMa NW without our measurements, and (3) is the model for Z CMa NW with additional scattered light that dominates at visual wavelengths and accounts for our measurements

wavelengths, it is not surprising that we find almost the same value for this parameter. By contrast, the inner disk radius is also constrained by the visible and UV data. As the contribution of Z CMa NW to the SED of Z CMa at visible wavelengths is not negligible, the SED of Z CMa SE at these wavelengths has to be lowered compared to the data used by KBGMN. This explains why we find a lower value for the disk inner radius.

The accretion rate is another widely used parameter to describe an accretion disk. Its value is related to the accretion power by:

$$L_{\rm acc} = \frac{GM_\star \dot{M}}{R_\star}. \qquad (3)$$

which leads to $\dot{M} \sim 5 \times 10^{-4} (M_\odot/M_\star)\, M_\odot\ {\rm yr}^{-1}$ in our model fit. Due to the difference in the fitted disk inner radius, KBGMN slightly overestimated the accretion rate and found $\dot{M} \sim 8 \times 10^{-4} (M_\odot/M_\star)\, M_\odot\ {\rm yr}^{-1}$.

3.2. The northwestern component

According to KBGMN, the SED of the northwestern component corresponds to the black body radiation of a spherical dust shell photosphere. Following this interpretation, we fitted the near-IR part of Z CMa NW spectrum by a black body and deduced a radius of $1690 \pm 30\, R_\odot$ and a luminosity of $2400 \pm 30\, L_\odot$ corresponding to a temperature of 980 K. This provides a good fit to the near-infrared data of KBGMN as shown by model curve number (2) in Fig. 2. The small difference between our values and those of KBGMN is explained by the fact that we take into account the interstellar extinction.

Such a black body spectrum, however, fails to reproduce the flux we measured for Z CMa NW at shorter wavelengths. In order to accommodate our measurements at 730 nm and 656 nm, the black body would have to be much hotter ($\simeq$ 1500 K) but would then fail to reproduce the near-IR part of the spectrum. In other words, as can be clearly seen from Fig. 2, the whole SED of Z CMa NW from 0.6 to 5 μm cannot be fitted by a single black body.

Since KBGMN model does not account for our observations at visible wavelengths, we tested two *simple* alternative models in the range 0.6-5 μm:

1. The data are compatible with a FU Orionis accretion disk model with the following parameters:

   $$\begin{aligned} L_\star &\quad \text{negligible} \\ L_{\rm acc} &= 3789 \pm 34\, L_\odot \\ R_{\rm min} &= 395 \pm 5\, R_\odot \\ \delta &= 1.4 \times 10^{-3} \pm 5 \times 10^{-5}\, R_\odot \end{aligned}$$

   where $R_{\rm min}$ is the inner disk radius and δ the thickness of the boundary layer. This model, however, implies an accretion rate of $\sim 5 \times 10^{-2}(M_\odot/M_\star)\, M_\odot\,{\rm yr}^{-1}$ leading to a time scale of only $\sim 20(M_\star/M_\odot)^2$ yr for the accretion phase. Consequently, this model must be rejected, unless this time scale can be shown to be characteristic of an FU Ori outburst (Bell & Lin 1994).
2. The excess flux at visible wavelengths from Z CMa NW compared to a black body dust sphere could arise from light originating from Z CMa SE scattered onto the dust photosphere surrounding Z CMa NW. In this case, the intensity ratio at visible wavelengths should be (neglecting the light directly produced by Z CMa NW in the visible):

   $$\frac{L_\lambda^{\rm NW}}{L_\lambda^{\rm SE}} = \eta_\lambda \frac{\pi R_{\rm sphere}^2}{4\pi\rho^2} \lesssim 1.4 \times 10^{-3}\eta_\lambda, \qquad (4)$$

   where ρ is the separation between the two components and η_λ is the scattering efficiency in the direction of the observer. If scattering follows Mie's law, then $\eta_\lambda \propto 1/\lambda$. Although this model provides a good fit to the data (see model curve number (3) in Fig. 2) it must be ruled out because the diffusion efficiency would have to be greater than unity ($\eta_{\rm V} \gtrsim 10^2$).

A variation on the last model may provide a plausible explanation for the observed flux excess associated with Z CMa NW at visible wavelengths. The good fit to the data provided by the last model strongly argues in favor of scattered light as the cause of the flux excess at 656 and 730 nm. As argued above, the scattered photons cannot originate from Z CMa SE for it would require an unreasonnable scattering efficiency. Instead, we assume that the photons come from Z CMa NW itself. We are thus led to interpret the spectral energy distribution of Z CMa NW as being the sum of 1) the black body emission arising from the dust photosphere of a circumstellar envelope, which accounts for the near-IR flux, and of 2) photons originating from the hidden central source which are scattered back into the line of sight, thus accounting for the visible flux excess. Scattering of the photons is assumed to take place along the walls of a cavity evacuated within the envelope. The existence of such a cavity in the envelope can be plausibly ascribed to a strong bipolar outflow which would originate from Z CMa NW, as evidenced by the large scale bipolar jets and HH objects observed around the system.

This interpretation implies that we are looking at Z CMa NW at a relatively low inclination, i.e., close enough to pole-on so that we do see the inner walls of the assumed bipolar cavity within the dusty envelope where the photons are scattered, but not quite pole-on so that the central source remains obscured by the asymmetric circumstellar dust distribution. Such a small inclination angle is independently supported by the large radial velocity of Z CMa's bipolar optical jets (up to 620 km s^{-1}, Poetzel et al. 1989) and by the modelling of Z CMa NW by KBGMN as an FU Ori disk seen pole-on (see also above).

Our interpretation of Z CMa's spectral energy distribution is further supported by the results of the spectropolarimetric study of the system by Whitney et al. (1993). These authors find that the emission lines in Z CMa's optical spectrum are more polarized than the continuum. They argue that the emission-line spectrum arises from Z CMa NW and that its high level of polarisation (6-8%) reveals that the central source is not directly visible but that we are indeed looking at scattered light. From a linear estimate of the polarisation function, they further predict that Z CMa NW contributes about 20% of the flux of the whole system at visible wavelengths. Given the fact that both components of the system are variable and that Whitney et al.'s and our observations are separated by 2 years, our *direct* measurement of a 15% contribution of Z CMa NW to the total flux of the system at 730 nm can be viewed as a neat confirmation of this model.

Finally, we note that quite similar results were recently obtained by Barth et al. (1994) using the same observational technique as the one used here but a different data analysis procedure. Not only the geometrical parameters they deduce for the system at visible wavelengths are in excellent agreement with ours, but also the flux ratio they measure between Z CMa NW and SE are the same as those derived here in spite of a 3 years interval between the two observations.

4. Conclusion

We have detected by speckle interferometry the visible counterpart of the so-called "infrared" companion of Z CMa discovered by Koresko et al. (1991). Our flux measurements for each component of the system at visible wavelengths does support Koresko et al.'s proposal that the "visible" SE component is a FU Ori accretion disk, but their model of a radiating dust sphere for the NW component is called into question. More specifically, we find that the NW component is much brighter at 656 and 730 nm than predicted by their model.

We have tried to fit the spectral energy distribution of each component of the Z CMa system from 0.3 to 5 μm by alternative models and conclude that the most plausible interpretation for the observed SED in that wavelength range is the following:

1. Z CMa SE is a FU Ori accretion disk seen nearly pole-on, as proposed by Koresko et al. (1991). This component contributes $\simeq$85% of the system luminosity at 730 nm.
2. Z CMa NW is hidden from view by a dusty asymmetric envelope. The dust photosphere of this envelope at a temperature of about 1000K dominates the near-IR flux of the system as proposed by Koresko et al. (1991). The dust photosphere has negligible contribution to the system flux at

visible wavelengths. Instead, we attribute the excess flux associated to Z CMa NW at these wavelengths to scattered light. We further argue that the scattered photons originate from Z CMa NW's central object, whose nature remains undefined, and are scattered back to the observer along the walls of a cavity evacuated in the dust envelope by a bipolar outflow.

Our observationnal results agree with those of Barth et al. (1994). Our interpretation matches independent constraints brought by the spectropolarimetric study of the system by Whitney et al. (1993).

References

Blazit A., 1987, PhD Thesis, Université de Nice (France).

Barth W., Weigelt G., Zinnecker H. 1994, A&A 291, 500

Bell K.R., Lin D.N.C. 1994, ApJ 427, 987

Bertout C., Basri G. & Bouvier J., 1988, ApJ, **330**, pp. 350–373.

Christou J.C., Cheng A.Y.S., Freeman J.D. & Roddier C., 1985, AJ **90**, 11, pp. 2644–2651.

Clariá J. J., 1974, Astron. Astrophys., **37**, pp. 229–236.

Demoment G., 1989, in *IEEE Transactions on Acoustics speech and Signal Processing* **37**, 12.

Devaney M.N., Thiébaut E., Foy R., Blazit A., Bonneau D., Bouvier J., de Batz B., Thom Ch., 1994, A&A, in press.

Foy, R., 1988a, in *Instrumentation for Ground-Based Optical Astronomy, Present and Future*, Robinson L. B. ed., Springer-Verlag (New-York), pp. 589–592.

Foy, R., 1988b, in *Instrumentation for Ground-Based Optical Astronomy, Present and Future*, Robinson L. B. ed., Springer-Verlag (New-York), pp. 345–359.

Haas M., Christou J. C., Zinnecker H., Ridgway S. T. & Leinert Ch., 1993, Astron. Astrophys., **269**, pp. 262–290.

Hartmann L., Kenyon S.J., Hewett R., Edwards S., Strom K.M., Strom S.E., Stauffer J.R., 1989, ApJ 338, 1001

Herbst W., Booth J. F., Koret D. L., Zajtseva G. V., Shakhovskaya N. I., Vrba F. J., Covino E., Terranegra L., A. Vittone, Hoff D., Kelsey L., Lines R. & Barksdale W., 1987, AJ, **94**, 1, pp. 137–149.

Hofmann K.-H., 1993, J. Opt. Soc. Am. A 10, p. 329.

Koresko C. D., Beckwith S. V. W., Ghez A. M., Matthews K. & Neugebauer G., 1991, AJ, **102**, 6, pp. 2073–2078 (KGBMN in the text).

Malbet F., Rigaut F., Léna P. & Bertout C., 1993, A&A **271**, L9-L12.

Poetzel R., Mundt R., Ray T.P. 1989, A&A 224, L13

Roddier F., Anuskiewicz J., Graves J.E., Northcott M. J. & Roddier C., 1994, SPIE 2201–01.

Tessier E., Bouvier J. & Lacombe F., 1994, A&A 283, 827.

Thiébaut E., 1994a, PhD Thesis, Université de Paris 7 (France).

Thiébaut E., 1994b, A&A **284**, 340.

Thiébaut E., Conan J.-M., 1995, J. Opt. Soc. Am. A **12**, 3.

Weigelt G., 1977, Opt. Commun. **21**, 55–59.

Whitney B.A., Clayton G.C., Shulte-Ladbeck R.E., Calvet N., Hartmann L., Kenyon S.J. 1993, ApJ 417, 687.

Wirnitzer B., 1985, J. Opt. Soc. Am. A **2**, 14–21.

This article was processed by the author using Springer-Verlag LaTeX A&A style file version 3.